Acta Crystallographica Section F
Structural Biology and Crystallization Communications
ISSN 1744-3091

Purification, crystallization and preliminary X-ray diffraction analysis of disease-related mutants of p97

Wai-Kwan Tang, Dongyang Li, Lothar Esser and Di Xia*

Laboratory of Cell Biology, Center for Cancer Research, National Cancer Institute, National Institutes of Health, Bethesda, Maryland 20892, USA

Correspondence e-mail: dixia@helix.nih.gov

Received 14 July 2009
Accepted 5 October 2009

The human type II AAA+ protein p97 participates in various cellular activities, presumably through its involvement in the ubiquitin–proteasome degradation pathway. Mutations in p97 have been implicated in patients with inclusion-body myopathy associated with Paget's disease of the bone and frontotemporal dementia (IBMPFD). In this work, three mutant p97 N-D1 fragments, R86A, R95G and R155H, were crystallized in the presence of ATPγS with PEG 3350 as a main precipitant, yielding two different crystal forms. The R155H mutant crystal belonged to space group $R3$, with unit-cell parameters in the hexagonal setting of $a = b = 134.2$, $c = 182.9$ Å, and was merohedrally twinned, with an estimated twin fraction of 0.34. The crystals of the R86A and R95G mutants belonged to space group $P1$, with similar unit-cell parameters of $a = 90.89$, $b = 102.6$, $c = 107.2$ Å, $\alpha = 97.5$, $\beta = 90.6$, $\gamma = 91.5^\circ$ and $a = 92.76$, $b = 103.7$, $c = 107.7$ Å, $\alpha = 97.7$, $\beta = 91.9$, $\gamma = 89.7^\circ$, respectively.

1. Introduction

Human p97 belongs to the AAA+ (extended family of ATPases associated with a variety of cellular activities) family of proteins, which hydrolyze ATP to induce conformational changes and use the resulting mechanical energy for substrate remodeling (Neuwald *et al.*, 1999). p97 belongs to the type II AAA+ proteins, featuring two AAA ATPase domains in tandem. It is highly abundant in the cytoplasm (Peters *et al.*, 1990) and takes part in various cellular pathways such as ER-associated degradation, homotypic membrane fusion and cell-cycle control, often with the assistance of various adaptor proteins such as p47 and Ufd1-Npl4 (Halawani & Latterich, 2006; Ye, 2006; Uchiyama & Kondo, 2005). Despite its apparent multivalent activities, p97 presumably carries out these functions through the ubiquitin–proteasome degradation pathway, in which p97 recognizes and shuttles polyubiquitinated proteins to proteasomes for degradation (Wang *et al.*, 2004). Autosomal inclusion-body myopathy associated with Paget's disease of the bone and frontotemporal dementia (IBMPFD) has been linked to mutations in p97 (Kimonis *et al.*, 2000). To date, mutations of p97 at positions Arg93, Arg95, Arg155, Gly157, Arg159, Arg191, Leu198, Ala232, Thr262 or Asn387 have been identified in patients with IBMPFD (Kimonis *et al.*, 2008; Djamshidian *et al.*, 2009). Inclusion bodies containing polyubiquitinated proteins and p97 have been found in tissues from IBMPFD patients, a fact that is consistent with the role of p97 in the ubiquitin–proteasome degradation pathway (Schroder *et al.*, 2005).

The structure of p97 consists of three domains. The N-terminal domain (N-domain) interacts with different protein partners such as p47 (Dreveny *et al.*, 2004) and Ufd1-Npl4 (Pye *et al.*, 2007), which allows p97 to function in different pathways. Following the N-domain are two tandem AAA ATPase domains, the D1-domain and the D2-domain, with linker regions between them. In the wild-type structures that have been determined of p97 (Zhang *et al.*, 2000; DeLaBarre & Brunger, 2003; Huyton *et al.*, 2003), the D1-domains and D2-domains form two stacked hexameric rings, with the N-domains radiating outward in the same plane as the D1-domain ring. Interestingly, in all the p97 structures published to date the D1-domains are always occupied by ADP, while the D2-domains are either bound with ADP–

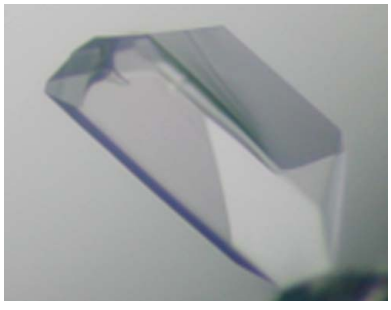

Table 1
Primers used in cloning and mutagenesis.

No.	Mutations	Direction	Sequence	Restriction site
1	Wt FL†	Forward	TGA**GGATCC**ATGGCTTCTGGAGCCGATTC	*Bam*HI
2	Wt FL†	Reverse	TCA**AGATCT**GCCATACAGGTCATCATCATTGTC	*Bgl*II
3	Wt N-D1	Forward	ACCTGGGAAGACATCGGGGGC**AGATCT**CATCACCATCACCATC	*Bgl*II
4	Wt N-D1	Reverse	GATGGTGATGGTGATG**AGATCT**GCCCCCGATGTCTTCCCAGGT	*Bgl*II
5	R53A	Forward	GAATTGCAGTTGTTCCGCGGTGACACAGTGTTGC	—
6	R53A	Reverse	GCAACACTGTGTCACCGCGGAACAACTGCAATTC	—
7	R86A	Forward	CTTGTTCTGATGAGAAGATTCGGATGAATGCTGTTGTTCGGAATAACCTTCG	—
8	R86A	Reverse	CGAAGGTTATTCCGAACAACAGCATTCATCCGAATCTTCTCATCAGAACAAG	—
9	R95G	Forward	GTTCGGAATAACCTTCGTGTAGGTCTAGGGGATGTCATCAGCATCC	—
10	R95G	Reverse	GGATGCTGATGACATCCCCTAGACCTACACGAAGGTTATTCCGAAC	—
11	R155H	Forward	GGAGACATTTTTCTTGTCCATGGTGGGATGCGTGCTGTG	—
12	R155H	Reverse	CACAGCACGCATCCCACCATGGACAAGAAAAATGTCTCC	—

† Wild-type full-length p97.

AlF_x or AMP-PNP or are nucleotide-free (Zhang *et al.*, 2000; DeLaBarre & Brunger, 2003, 2005; Huyton *et al.*, 2003). To understand how IBMPFD mutations might affect the structure and function of p97, we purified three N-D1 fragments of p97 bearing the IBMPFD mutations R86A, R95G and R155H, and crystallized each in the presence of ATPγS.

2. Materials and methods

2.1. Construction of wild-type p97 and IBMPFD mutant p97 N-D1 expression plasmids

The DNA fragment encoding full-length p97 was amplified from a p97 clone (accession No. BC110913) available from Thermo Scientific (Huntsville, Alabama, USA) using the first primer pair listed in Table 1 (Nos. 1 and 2). The primers contain restriction sites for *Bam*HI and *Bgl*II, respectively. The PCR product was cloned into a pQE60 expression vector (Qiagen, Valencia, California, USA) through the *Bam*HI/*Bgl*II sites, generating the expression plasmid pQE-p97. A hexahistidine-affinity tag was attached to the C-terminus of p97 *via* a two-residue linker Arg-Ser (RSH_6 tag). The p97 DNA fragment encoding Met1–Gly481 (N-D1 fragment) was then generated by deletion mutagenesis, removing residues 482–806 from the plasmid pQE-p97, by using the QuikChange site-directed mutagenesis kit (Stratagene, La Jolla, California, USA) with the second primer pair (Nos. 3 and 4) listed in Table 1. The resulting PCR product is the expression plasmid pQE-p97ND1 containing the wild-type p97 N-D1 fragment inserted between *Bam*HI/*Bgl*II sites in the pQE60 vector with a C-terminal RSH_6 affinity tag. The N-D1 fragments for mutants R86A, R95G and R155H were obtained using the QuikChange site-directed mutagenesis kit with the primer pairs listed in Table 1. Constructs were confirmed by DNA sequencing.

2.2. Expression and purification of p97 N-D1 fragments

Expression plasmids were transformed into *Escherichia coli* strain M15 (QIAexpression system, Qiagen). Transformed cells were grown at 310 K in Terrific Broth supplemented with 100 µg ml^{-1} ampicillin and 50 µg ml^{-1} kanamycin and were induced by 1 m*M* isopropyl β-D-1-thiogalactopyranoside at an OD_{600} of 1.0. Cells were harvested by centrifugation and the pellet was resuspended in buffer *A* (25 m*M* Tris–HCl pH 7.6, 0.3 m*M* NaCl, 10 m*M* imidazole and 0.25 m*M* DTT) supplemented with a protease-inhibitor cocktail (Santa Cruz Biotechnology, Santa Cruz, California, USA). Cells were lysed by sonication followed by centrifugation to remove cell debris at 15 000*g* for 40 min at 277 K. Subsequently, the supernatant was incubated with Ni–NTA resin (Qiagen) pre-equilibrated with buffer *A* for 1 h at 277 K. Unbound materials were washed away in two steps with buffer *A* supplemented with 50 m*M* and then 100 m*M* imidazole and bound proteins were eluted with 250 m*M* imidazole in buffer *A*. After elution, proteins were concentrated, dialyzed against a buffer containing 20 m*M* Tris–HCl pH 8.0, 10% glycerol and stored at 193 K until use. All proteins were purified using the same procedure. The hexahistidine tag remained uncleaved at the C-terminus in all purified proteins. The protein concentration was determined using BCA methods (Smith *et al.*, 1985).

2.3. Oligomeric state of p97 N-D1 fragments

The oligomeric states of the p97 variants were analyzed by both native gel electrophoresis using blue native PAGE (Invitrogen, Carlsbad, California, USA) and gel-filtration chromatography using a Superdex 200 column (GE Healthcare, Piscataway, New Jersey, USA) in a buffer containing 20 m*M* Tris–HCl pH 8.0 and 10% glycerol.

2.4. Crystallization of mutant p97 N-D1 fragments

Prior to crystallization trials, all protein samples were first treated with 5 m*M* DTT followed by the addition of $MgCl_2$ and ATPγS to final concentrations of 40 and 4 m*M*, respectively. The mixture was centrifuged at 12 600*g* for 1 h and the supernatant was used for crystallization. Mutant p97 N-D1 fragments were crystallized by the hanging-drop vapor-diffusion method at 288 K. Typically, for each mutant an initial crystallization screening was performed robotically with a Mosquito automated solution dispenser (TTP LabTech, Royston, England) using commercially available high-throughput screening kits (from Sigma, Hampton Research and Molecular Dimensions) in hanging-drop format. Each droplet consisted of a mixture of 300 nl protein solution and 300 nl reservoir solution and was equilibrated over 50 µl reservoir solution. The conditions that yielded initial hits were repeated and confirmed with solutions prepared in-house.

2.5. Cryoprotection and X-ray diffraction data collection

The crystals of the p97 N-D1 mutants were fragile and difficult to freeze cryogenically. A large number of cryoprotection agents such as glycerol, various ethylene glycols, Paratone oil mixtures *etc.* were screened to search for the best conditions. Only a few crystals survived the treatment while retaining sufficient diffraction resolution for the collection of complete data sets. Mutant p97 crystals consistently performed better on soaking them for 3 min in buffer solutions containing 10 m*M* Tris–HCl pH 8.0, 2% benzamidine, 50 m*M* citrate buffer pH 5.8, 20 m*M* $MgCl_2$, 5 m*M* DTT, 20% PEG 3350 with increasing amounts of glycerol. This stepwise process

Table 2
Statistics for the quality of diffraction data sets for mutant p97.

All data sets were collected on SERCAT beamline ID22 at Argonne National Laboratory. Values in parentheses are for the last shell.

Data set	R155H	R95G	R86A
Space group	*R*3†	*P*1	*P*1
Bound nucleotide	ATPγS	ATPγS	ATPγS
Unit-cell parameters (Å, °)	$a = b = 134.2$, $c = 182.9$†	$a = 92.76$, $b = 103.3$, $c = 107.7$, $\alpha = 97.7$, $\beta = 91.9$, $\gamma = 89.7$	$a = 90.89$, $b = 102.6$, $c = 107.2$, $\alpha = 97.5$, $\beta = 90.6$, $\gamma = 91.5$
Resolution (Å)	50–2.1 (2.23–2.10)	50–2.8 (2.90–2.80)	50–2.85 (2.95–2.85)
Mosaicity (°)	0.76	0.82	0.96
No. of observations	235711	151406	200205
No. of unique reflections	66557	87240	85163
Completeness (%)	99.5 (95.6)	90.5 (71.5)	91.8 (67.8)
$R_{\rm merge}$‡	0.057 (0.524)	0.050 (0.493)	0.049 (0.502)
$I/\sigma(I)$	19.7 (1.7)	12.3 (0.8)	13.8 (1.02)
Phasing			
Model used	PDB entry 1e32	R155H N-D1 fragment	R155H N-D1 fragment
Log-likelihood gain	446§	5792¶	6717¶
R in initial rigid-body refinement	0.43	0.38	0.37
FOM	0.36	0.59	0.62

† *R*3 space group in hexagonal setting. ‡ $R_{\rm merge}$ is defined as $\sum_{hkl}\sum_i |I_i(hkl) - \langle I(hkl)\rangle|/\sum_{hkl}\sum_i I_i(hkl)$, where $I_i(hkl)$ is the intensity of the *i*th observation of a reflection with Miller indices *hkl* and $\langle I(hkl)\rangle$ is the mean intensity for all measured $I(hkl)$ and Friedel pairs. § MR was performed with *Phaser* using the automatic MR option. Two PDB files were provided: one for the D1-domain and another for the N-domain. We asked for two copies each of the D1-domain and N-domain. A single solution was obtained. A search with an intact N-D1 from PDB entry 1e32 produced a wrong solution with a log-likelihood gain of −42. ¶ A monomeric N-D1 fragment from the R155H mutant structure was used as a phasing model, asking for six N-D1 subunits in a crystallographic asymmetric unit. A single solution was obtained.

(typically 15 steps) continued until a final concentration of 28% glycerol was reached. The crystals were then flash-frozen in liquid propane.

X-ray diffraction experiments were carried out at 100 K on the SER-CAT (ID-22) beamline at the Advanced Photon Source at Argonne National Laboratory. Diffraction images were collected with a MAR 225 CCD detector and processed and scaled with the *HKL*-2000 package (Otwinowski & Minor, 1997). Statistics of X-ray diffraction data collection and for the qualities of data sets are given in Table 2.

2.6. Structure determination of the N-D1 mutants

The structure of the R155H mutant with bound ATPγS was determined by molecular replacement (MR) using the program *Phaser* (Storoni *et al.*, 2004). Merohedral twinning in the data set was detected using the twinning server (http://nihserver.mbi.ucla.edu/Twinning; Yeates, 1997) and the data set was detwinned using the program *DETWIN* in the *CCP*4 program package (Collaborative Computational Project, Number 4, 1994). The structure was further refined with the program *REFMAC* (Murshudov *et al.*, 1997) using the detwinned data set. Bound ligands were inserted manually with the graphical modeling program *O* (Jones *et al.*, 1991). The structures of both the R95G and R86A mutants in the ATPγS-bound form were also solved with *Phaser* using a monomeric template from the R155H mutant as a search model.

3. Results and discussion

Three wild-type structures of p97 are available and all are hexameric: one is an N-D1 fragment (Zhang *et al.*, 2000) and the other two are full-length proteins (DeLaBarre & Brunger, 2003; Huyton *et al.*, 2003). Interestingly, ADP molecules are bound to the D1-domains in all of them, regardless of the nucleotide form used for crystallization. In the present study, three N-D1 fragments of IBMPFD mutant p97 (R86A, R95G and R155H) were crystallized in the presence of ATPγS and their structures were determined, with a highest resolution of 2.1 Å.

3.1. Mutant p97 N-D1 fragments form hexamers in solution

Purified mutant proteins were subjected to blue native PAGE analysis (Ma & Xia, 2008; Wittig *et al.*, 2006). All mutants formed hexamers in solution, with an estimated molecular weight of 333.6 kDa (Fig. 1*a*), suggesting that they behave just like the wild-type N-D1 fragment. When subjected to SDS–PAGE analysis, the same protein migrated as monomers with a molecular weight of 54.5 kDa (Fig. 1*b*).

3.2. p97 mutants crystallize in two different crystal forms

Our robotic screens began with the R155H mutant N-D1 at a protein concentration of 10 mg ml^{-1} in a buffer containing 20 m*M* Tris–HCl pH 8.0 and 20% glycerol. An initial set of conditions was identified from the Sigma HT screen kit, which gave rise to small crystals (condition A9; 0.2 *M* ammonium acetate, 0.1 m*M* sodium citrate pH 5.6 and 30% PEG 4000). This set of conditions was subsequently refined with various PEG and additive screens. The best crystals for the R155H mutant were obtained by mixing the protein (7 mg ml^{-1} in 20 m*M* Tris–HCl pH 8.0, 40 m*M* $MgCl_2$, 4 m*M* ATPγS, 5 m*M* DTT and 10% glycerol) in a 1:1 ratio with a reservoir solution containing 0.1 *M* citrate buffer pH 5.6, 6% benzamidine, 7% PEG 3350 and 20% glycerol. Similarly, crystals of the R95G mutant were obtained by mixing the protein (5 mg ml^{-1} in 10 m*M* Tris–HCl pH 8.0, 40 m*M* $MgCl_2$, 4 m*M* ATPγS, 5 m*M* DTT and 10% glycerol) in an equal ratio with a reservoir solution consisting of 0.1 *M* citrate buffer pH 5.7, 0.1 *M* NaCl, 13.5% PEG 3350 and 20% glycerol. The R86A mutant (5 mg ml^{-1} in 20 m*M* Tris–HCl pH 8.0, 40 m*M* $MgCl_2$, 4 m*M* ATPγS, 5 m*M* DTT and 10% glycerol) was crystallized with a well

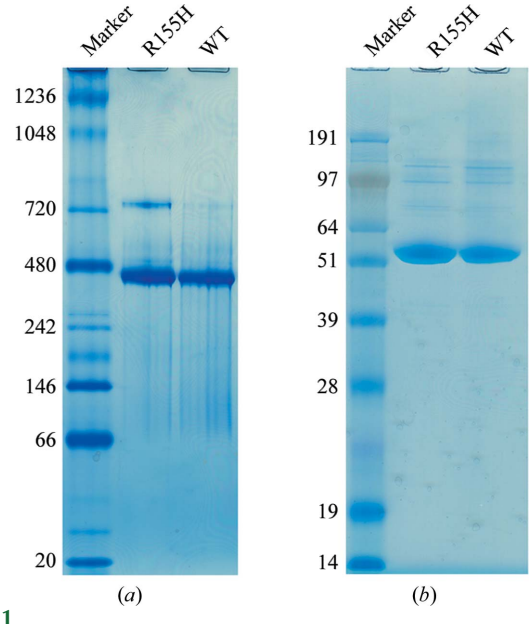

Figure 1
Oligomeric states of purified N-D1 fragments of p97 mutant R155H. (*a*) Blue native PAGE analysis with NativeMarker (Invitrogen) as molecular-weight standards. (*b*) SDS–PAGE analysis with SeeBlue-Plus2 (Invitrogen) as molecular-weight standards.

solution containing 0.1 *M* citrate buffer pH 5.8, 0.1 *M* NaCl, 4% benzamidine, 16.5% PEG 3350 and 20% glycerol. Crystals appeared a few days after setup and reached full size (0.1–0.2 mm) in about 2–3 weeks in hanging drops.

After treatment with cryoprotectant, the mutant p97 crystals were frozen in liquid propane and subjected to an X-ray diffraction screen. Most crystals were not protected well by the procedures described in §2 and diffracted X-rays poorly. Occasionally, crystals diffracted to 3 Å resolution or better and complete data sets were collected. R155H mutant crystals could grow to substantial sizes (Fig. 2*a*) and displayed the symmetry of space group *R*3. The best R155H mutant crystal we obtained diffracted X-rays to 2.1 Å resolution (Table 2). There are two copies of N-D1 in the asymmetric unit, giving rise to a Matthews coefficient (V_M) of 2.96 Å^3 Da^{-1}, corresponding to a

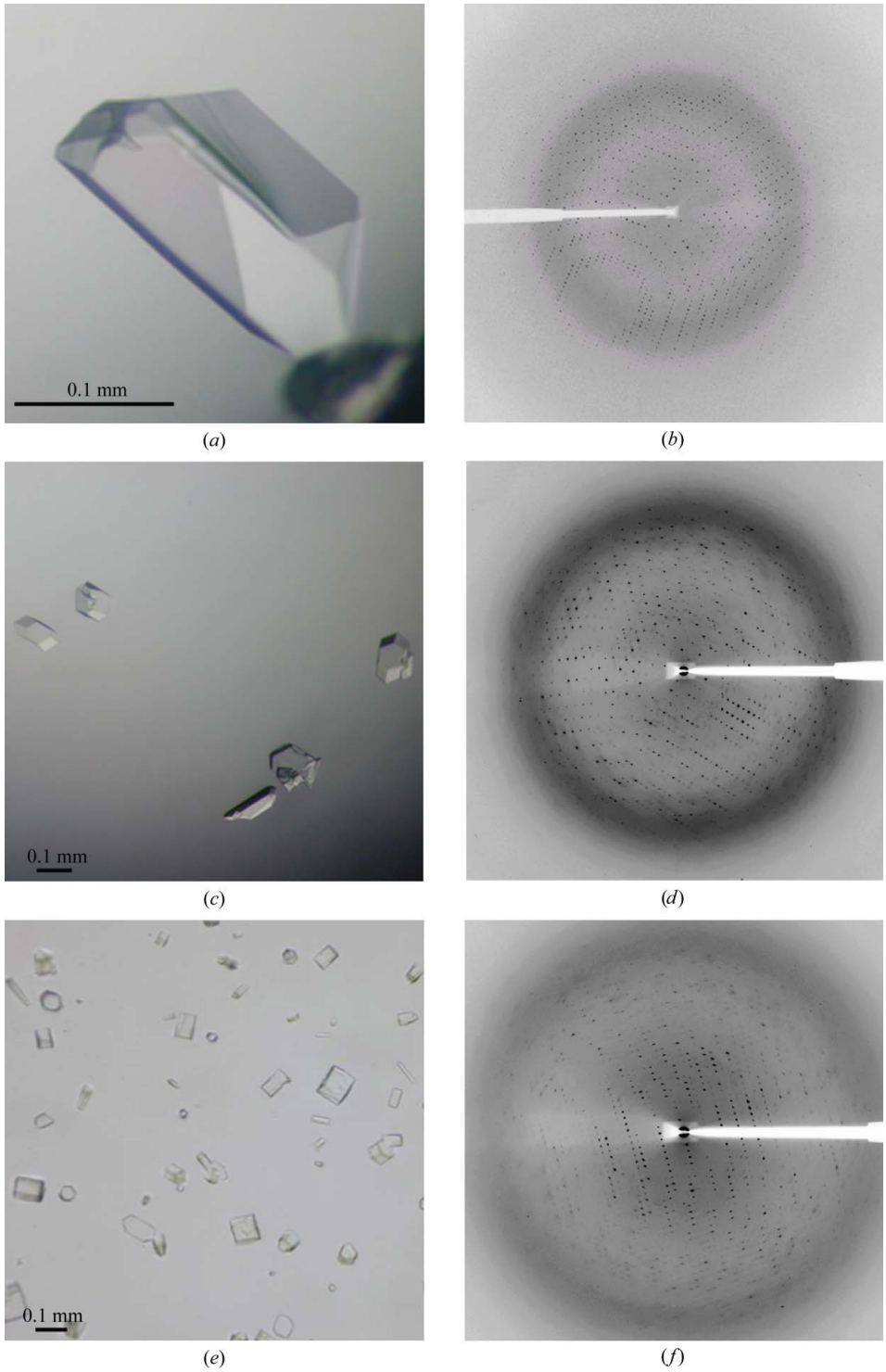

Figure 2
Crystals and X-ray diffraction patterns for N-D1 fragments of p97 mutants. (*a*) Typical crystals of the R155H mutant grown in the presence of ATPγS. (*b*) X-ray diffraction pattern of an R155H mutant crystal. (*c*) Crystals of the R95G mutant grown in the presence of ATPγS. (*d*) Diffraction image of an R95G mutant crystal. (*e*) Crystals of the R86A mutant grown in the presence of ATPγS. (*f*) Diffraction pattern of an R86A mutant crystal.

solvent content of 58% (Matthews, 1968). Both the R95G and R86A mutant crystals behaved much more poorly than those of R155H in diffraction experiments, diffracting X-rays to only 2.8 and 2.85 Å resolution, respectively. They have very similar unit-cell parameters with one hexamer in the unit cell, corresponding to a V_M value of 3.19 $Å^3$ Da^{-1} and a solvent content of 61%. Statistics of data collection and data quality are given in Table 2.

3.3. Structure solution of the R155H mutant in the presence of merohedral twinning

We began our structure determination with the data set from the R155H mutant crystal because it had the highest resolution. Molecular replacement (MR) using a model template based on the wild-type N-D1 fragment with bound ADP (PDB code 1e32; Zhang *et al.*, 2000) failed to yield successful solutions for the expected two NCS-related copies. Assuming that the mutations and/or the presence of ATPγS might have changed the relative positions of the N-domain and D1-domain, we carried out MR using separate templates for the N-domain and D1-domain and found two solutions for each domain. The structure was subsequently refined and rebuilt in many cycles with the addition of new features, but the free *R* value remained high at approximately 38%. The existence of merohedral twinning in the *R*3 crystal was detected; the data set was detwinned with an initial estimated twin fraction of 0.34 and a twin operator of $k, -h, l$ (in the hexagonal setting). Structure refinement against the detwinned data set is in progress.

3.4. Structure determination of the R86A and R95G mutants by molecular replacement

The structures of both the R95G and R86A mutants in the ATPγS-bound form were solved by molecular replacement with *Phaser* using a monomeric template from the high-resolution R155H mutant as a search model. Six copies of the p97 N-D1 protomer are present in the unit cell. Structure refinement and analysis of the two mutants of p97 with ATPγS bound are in progress.

The authors wish to thank the staff members of the SER-CAT beamline (ID-22) at Advanced Photon Source, Argonne National Laboratory for their assistance in data collection. We also thank George Leiman for editorial assistance. This research was supported by the Intramural Research Program of the NIH, National Cancer Institute, Center for Cancer Research.

References

Collaborative Computational Project, Number 4 (1994). *Acta Cryst.* D**50**, 760–763.
DeLaBarre, B. & Brunger, A. T. (2003). *Nature Struct. Biol.* **10**, 856–863.
DeLaBarre, B. & Brunger, A. T. (2005). *J. Mol. Biol.* **347**, 437–452.
Djamshidian, A., Schaefer, J., Haubenberger, D., Stogmann, E., Zimprich, F., Auff, E. & Zimprich, A. (2009). *Muscle Nerve*, **39**, 389–391.
Dreveny, I., Kondo, H., Uchiyama, K., Shaw, A., Zhang, X. & Freemont, P. S. (2004). *EMBO J.* **23**, 1030–1039.
Halawani, D. & Latterich, M. (2006). *Mol. Cell*, **22**, 713–717.
Huyton, T., Pye, V. E., Briggs, L. C., Flynn, T. C., Beuron, F., Kondo, H., Ma, J., Zhang, X. & Freemont, P. S. (2003). *J. Struct. Biol.* **144**, 337–348.
Jones, T. A., Zou, J.-Y., Cowan, S. W. & Kjeldgaard, M. (1991). *Acta Cryst.* A**47**, 110–119.
Kimonis, V. E., Fulchiero, E., Vesa, J. & Watts, G. (2008). *Biochim. Biophys. Acta*, **1782**, 744–748.
Kimonis, V. E., Kovach, M. J., Waggoner, B., Leal, S., Salam, A., Rimer, L., Davis, K., Khardori, R. & Gelber, D. (2000). *Genet. Med.* **2**, 232–241.
Ma, J. & Xia, D. (2008). *J. Appl. Cryst.* **41**, 1150–1160.
Matthews, B. W. (1968). *J. Mol. Biol.* **33**, 491–497.
Murshudov, G. N., Vagin, A. A. & Dodson, E. J. (1997). *Acta Cryst.* D**53**, 240–255.
Neuwald, A. F., Aravind, L., Spouge, J. L. & Koonin, E. V. (1999). *Genome Res.* **9**, 27–43.
Otwinowski, Z. & Minor, W. (1997). *Methods Enzymol.* **276**, 307–326.
Peters, J. M., Walsh, M. J. & Franke, W. W. (1990). *EMBO J.* **9**, 1757–1767.
Pye, V. E., Beuron, F., Keetch, C. A., McKeown, C., Robinson, C. V., Meyeer, H. H., Zhang, X. & Freemont, P. S. (2007). *Proc. Natl Acad. Sci. USA*, **104**, 467–472.
Schroder, R., Watts, G. D., Mehta, S. G., Evert, B. O., Broich, P., Fliessbach, K., Pauls, K., Hans, V. H., Kimonis, V. & Thal, D. R. (2005). *Ann. Neurol.* **57**, 457–461.
Smith, P. K., Krohn, R. I., Hermanson, G. T., Mallia, A. K., Gartner, F. H., Provenzano, M. D., Fujimoto, E. K., Goeke, N. M., Olson, B. J. & Klenk, D. C. (1985). *Anal. Biochem.* **150**, 76–85.
Storoni, L. C., McCoy, A. J. & Read, R. J. (2004). *Acta Cryst.* D**60**, 432–438.
Uchiyama, K. & Kondo, H. (2005). *J. Biochem.* **137**, 115–119.
Wang, Q., Song, C. & Li, C. (2004). *J. Struct. Biol.* **146**, 44–57.
Wittig, I., Braun, H. P. & Schagger, H. (2006). *Nature Protoc.* **1**, 418–428.
Ye, Y. (2006). *J. Struct. Biol.* **156**, 29–40.
Yeates, T. O. (1997). *Methods Enzymol.* **276**, 344–358.
Zhang, X., Shaw, A., Bates, P. A., Newman, R. H., Gowen, B., Orlova, E., Gorman, M. A., Kondo, H., Dokurno, P., Lally, J., Leonard, G., Meyer, H., van Heel, M. & Freemont, P. S. (2000). *Mol. Cell*, **6**, 1473–1484.